Energy Efficiency Analysis of Coherent Links for Datacenters

Takako Hirokawa[1], Sergio Pinna[1], Jonathan Klamkin[1], James F. Buckwalter[1], and Clint L. Schow[1]

***Abstract*— We propose that coherent optical communication can offer energy-efficient operation in datacenters. Analysis and simulations determine optimal operating points for the laser and local oscillator (LO) and compare trade-offs in Silicon (Si) and Indium Phosphide (InP) Mach-Zehnder Modulators (MZMs) to reach pJ/b scale efficiency.**

I. Introduction

Cloud-based data storage, high performance computing, audio and video streaming services etc., base their operations on mega-datacenters. The energy consumption of such infrastructure is becoming a significant part of the total U.S. energy bill. In 2014, the estimated energy consumption of datacenters in the United States reached 70TWh, roughly 1.8% of the total consumption [1]. Globally in 2025, datacenters are expected to consume over 3000TWh, an increase of a factor of about 15 from 203 TWh in 2015 [2]. Therefore, more research is required to optimize energy efficiency in datacenters.

The energy consumption of a long-haul QPSK coherent link has been previously analyzed in [3]. We analyze integrated circuit technology factors that impact energy efficiency in a quadrature phase shift keying (QPSK) coherent optical link based on an optical phase-locked loop (OPLL) [4]. Starting from the model of a coherent link, we analyze the necessary source and LO optical and electrical driver power requirements.

II. Coherent Model

The coherent link model consists of a QPSK transmitter, a low-loss optical link (<2km), and a homodyne coherent receiver. We considered two modulator types and two photonic integrated circuit (PIC) platforms. The first modulator type is based on a traveling wave modulator (TW-MZM) architecture [5], while the second, on a segmented modulator (SEG-MZM) architecture [6]. Both architectures have been considered in both Si and InP platforms. We find that the choice of transmitter (TX) type and PIC technology has a significant impact on the overall link performance and power budget.

A QPSK signal is realized when the MZM is biased at the null point, where the electric field transmission is 0. At this bias point, the optical carrier undergoes a 180°phase shift when the MZM is driven by differential signals in a push-pull configuration even when the voltage swing is less than the full modulator half wave voltage (V_π) of the MZM. The modulation factor (F_M) is the ratio between the voltage driving the MZM relative to $2V_\pi$ of the MZM. It determines the optical loss through the MZM and therefore the required source laser power, and the power consumed by the TX driver and modulator to generate the level of modulation.

$$F_M = \frac{1}{2}\left(1+\cos\left(\pi\frac{V_{sig}}{2V_\pi}\right)\right) \tag{1}$$

where V_{sig} is the total drive voltage. Note that a F_M of 1, which corresponds to a $2V_\pi$ voltage swing, leads to no modulation induced loss, while F_M of 0.5 corresponds to a V_π voltage swing and induces 3dB of optical loss. The loss due to the modulation is therefore controlled by the drive voltage amplitude while propagation losses through the MZM exist independently.

*email: hirokawat@ece.ucsb.edu

[1]Electrical and Computer Engineering, University of California Santa Barbara

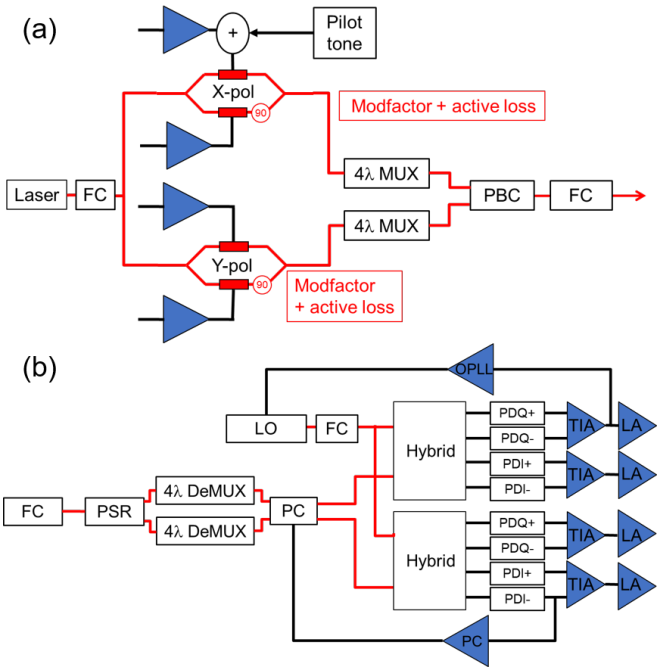

Fig. 1. Schematics for the TX (a) and RX (b). The red lines represent the optical path, while the black lines represent the electrical lines. For the InP system, the fiber-to-chip coupler (FC) after the laser and LO is left out as we assume that the laser can be fabricated on chip. PBC = polarization beam splitter.

At the receiver, the bit error rate (BER) is determined by the SNR. For homodyne coherent detection, [7]

$$\mathrm{SNR} = \frac{\langle I_{ac}^2\rangle}{\sigma^2} = \frac{4R^2AP_{laser}P_{LO}}{2qR\Delta f(P_{LO}+AP_{laser}+I_d/R)+\sigma_T^2} \tag{2}$$

Here P_{laser} is the optical power from the source laser at the TX input, P_{LO} is the optical power of the LO at the photodetector, A is the total link attenuation, R and I_d are, respectively, the detector responsivity and dark current, σ_T^2 is the thermal noise variance. In our model, F_M-induced losses are included in the total link attenuation, A. For PSK detection, the Q is the square root of the SNR and is directly related to the link BER. We targeted a BER =10^{-12}, or Q = 7.

Figure 1 illustrates a detailed schematic of the QPSK coherent link considered in the model for the Si-based architectures. Other technology-dependent losses, such as waveguide passive attenuation, are also included in the model.

III. Results and Discussion

Our modeling tool is used to explore the coherent link design space of modulator length, drive voltage, and laser powers, both source and LO. In the link simulations, we utilize differential drive for both the SEG-MZM and TW-MZMs, and use polarization multiplexing to increase the link capacity by a factor of 2. These calculations include all sources of power dissipation in the link, including the TX and LO lasers, MZM

978-1-7281-1496-5/19/$31.00 ©2019 IEEE

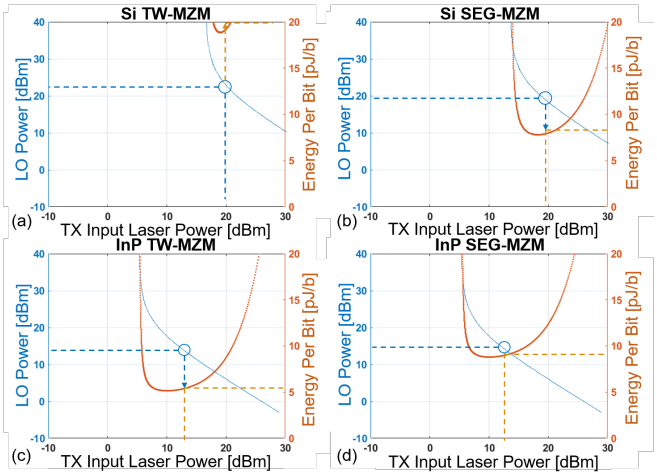

Fig. 2. Simulation results for a 6-mm-long Si TX/Si RX are shown in (a) and (b) and a 2-mm-long InP TX/Si RX are shown in (c) and (d). V_{sig} are (a) 1.2V, (b) 2.2V, and 0.9V in (c) and (d). The EPB curve (red) and LO power curve (blue) correspond to Q = 7 (BER = 10^{-12}).

driver and RX circuits, and OPLL and polarization control loops. The circuit power dissipation numbers are extracted from transistor-level Cadence simulations. The plots show design parameters that achieve sub-10pJ/bit energy efficiency for MZMs of practical lengths, and illustrate the trade-off between MZM length and drive voltage on link efficiency in energy per bit (EPB). In all of the simulations that follow, unless otherwise noted, the link margin is set to 13 dB.

Figure 2(a,b) guides operating conditions for a link operating at 10^{-12} BER for 6-mm long Si MZMs. In general, the EPB decreases with MZM length. A 6-mm Si MZM reaches the limit of feasibility from a density and packaging perspective and considering traveling wave electrode losses. While sub-10pJ/bit operation is possible with TW-MZMs, the SEG-MZM implementation is considerably less efficient, on the order of 19 pJ/bit. Furthermore, from a practical standpoint, operating the LO and the TX lasers at power levels higher than 16 dBm (40 mW) may not be feasible. Finding a point along the LO power curve that balances the input and LO laser powers indicates around 18 dBm is required for both the LO and TX for the TW-MZM and 21 dBm for the SEG-MZM. For Si, we have assumed that $V_\pi L_\pi$ = 15 V-mm. In estimating the TX loss, we included the passive optical loss of the waveguides due to undoped and doped sections as well as the splitters and couplers. To calculate the capacitance and modulation efficiency of the pn junction phase shifters, capacitance and $V_\pi L_\pi$ values consistent with reports in the literature were used [8]. The laser efficiency was set to 20%. To estimate parameters in InP, we have used a combination of simulations and knowledge due to prior work. While it is possible to achieve low EPB, Si TXs have high loss due to inefficient MZMs that degrades link efficiency and drives laser power requirements to challenging, if not unrealistic levels.

The outlook improves for InP TXs regarding both link efficiency and laser power requirements. Figure 2(c,d) shows the simulation output for a 2-mm long InP modulator driven with 0.9V. Since sub-10pJ/bit operation is much easier with an InP TX, we constrained the design space further by choosing a drive voltage corresponding to V_π for a 2-mm long device. For the InP simulations, we model $V_\pi L_\pi$ as 2 V-mm. The InP design point is very realizable, requiring only 1 V differential drivers and less than +13 dBm from both the input and LO

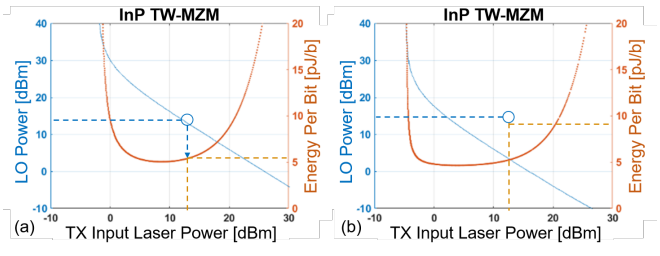

Fig. 3. Starting from the conditions used to generate Figure 2(c), LO and EPB vs TX power for (a) BER 10^{-3} and (b) 3dB link margin cases are shown.

lasers. Note that although InP TXs offer a much more efficient solution, on the RX side a Si implementation may be more favorable as polarization de-multiplexing is more feasible. All of the simulations in this section incorporate a Si RX PIC.

To further explore the design space, simulations were conducted at reduced BER and link budget. Allowing the BER to increase to 10^{-3}—which would require forward error correction (FEC)—has minor impacts on the EPB and laser power requirements, favoring operation at native error rates of 10^{-12}. Figure 3(b) demonstrates that the EPB does not change appreciably, but the required LO and input laser powers are reduced to around +9 dBm.

IV. Conclusion

A comprehensive QPSK coherent link model has been presented and indicates that EPB under 10pJ/bit is possible with substantial improvements in SNR. The simulation tool allows exploration of optical and electrical parameters that impact PIC design. Measured hardware will verify and refine the parameters used in the link analysis.

Acknowledgments

The information, data, or work presented herein was funded in part by the Advanced Research Projects Agency-Energy (ARPA-E), U.S. Department of Energy, under Award Number DE-AR0000848. The views and opinions of authors expressed herein do not necessarily state or reflect those of the United States Government or any agency thereof.

References

[1] A. Shehabi, S. J. Smith, D. A. Sartor, R. E. Brown, M. Herrlin, J. G. Koomey, E. R. Masanet, N. Horner, I. L. Azevedo, and W. Lintner, "United states data center energy usage report," tech. rep., Berkeley Lab, 06 2016.

[2] *Total Consumer Power Consumption Forecast*, 2017.

[3] B. S. G. Pillai, B. Sedighi, K. Guan, N. P. Anthapadmanabhan, W. Shieh, K. J. Hinton, and R. S. Tucker, "End-to-end energy modeling and analysis of long-haul coherent transmission systems," *Journal of Lightwave Technology*, vol. 32, pp. 3093–3111, Sep. 2014.

[4] S. Ristic, A. Bhardwaj, M. J. Rodwell, L. A. Coldren, and L. A. Johansson, "An optical phase-locked loop photonic integrated circuit," *Journal of Lightwave Technology*, vol. 28, pp. 526–538, Feb 2010.

[5] M. Streshinsky, R. Ding, Y. Liu, A. Novack, Y. Yang, Y. Ma, X. Tu, E. K. S. Chee, A. E.-J. Lim, P. G.-Q. Lo, T. Baehr-Jones, and M. Hochberg, "Low power 50 gb/s silicon traveling wave mach-zehnder modulator near 1300 nm," *Opt. Express*, vol. 21, pp. 30350–30357, Dec 2013.

[6] B. G. Lee, N. Dupuis, R. Rimolo-Donadio, T. N. Huynh, C. W. Baks, D. M. Gill, and W. M. J. Green, "Driver-integrated 56-gb/s segmented electrode silicon mach zehnder modulator using optical-domain equalization," in *Optical Fiber Communication Conference*, p. Th1B.1, Optical Society of America, 2017.

[7] G. P. Agrawal, *Fiber-Optic Communication Systems*. John Wiley Sons, Inc, fourth ed., 2010.

[8] H. Yu, M. Pantouvaki, J. V. Campenhout, D. Korn, K. Komorowska, P. Dumon, Y. Li, P. Verheyen, P. Absil, L. Alloatti, D. Hillerkuss, J. Leuthold, R. Baets, and W. Bogaerts, "Performance tradeoff between lateral and interdigitated doping patterns for high speed carrier-depletion based silicon modulators," *Opt. Express*, vol. 20, pp. 12926–12938, Jun 2012.